heating by solar electromagnetic induction has gained favor with the recognition of a sun-centered heating pattern in the asteroid belt, that model is highly simplified (for example, it assumes a time-independent magnetic field, axisymmetry of electric potential within the target object, and the validity of a first-term truncation of the Legendre series solution) and contains considerable uncertainties in parameter choices (early solar electric and magnetic flux, strong temperature, and compositional dependence of electrical conductivity) (*17*). We cannot reject this hypothesis with present data, but we favor ^{26}Al heating because it can explain the observed data with fewer assumptions and because ^{26}Al is known to have been present in significant quantities in newly accreted meteorite parent bodies (*4*).

REFERENCES AND NOTES

1. C. P. Sonett and R. T. Reynolds, in *Asteroids*, T. Gehrels, Ed. (Univ. of Arizona Press, Tucson, 1979), pp. 822–848.
2. J. A. Wood and P. Pellas, in *The Sun in Time*, C. P. Sonett, M. S. Giampapa, M. S. Matthews, Eds. (Univ. of Arizona Press, Tucson, 1992), pp. 740–760.
3. T. Lee, D. A. Papanastassiou, G. J. Wasserburg, *Geophys. Res. Lett.* **3**, 109 (1976).
4. I. D. Hutcheon, R. Hutchison, G. J. Wasserburg, *Nature* **337**, 238 (1989).
5. E. Zinner and C. Gopel, *Meteoritics* **27**, 311 (1992).
6. M. Miyamoto, N. Fujii, H. Takeda, *Proc. Lunar Planet. Sci. Conf.* **12B**, 1145 (1981).
7. R. E. Grimm and H. Y. McSween, Jr., *Icarus* **82**, 244 (1989).
8. M. Miyamoto, *Meteoritics* **26**, 111 (1991).
9. A. Shukolyukov and G. W. Lugmair, *Lunar Planet. Sci.* **XXIII**, 1295 (1992).
10. The initial ^{26}Al to ^{27}Al ratio in CAIs (*3*) was reported to be 6×10^{-5}, whereas the initial ^{60}Fe to ^{56}Fe ratio in CAIs (*9*) was inferred to be 1.6×10^{-6}. The decay energies are both about 3 MeV per atom, and the half-lives are 0.72 million years for ^{26}Al and 1.5 million years for ^{60}Fe. Assuming these proportions were incorporated into carbonaceous chondrites with 210 mg of bulk Fe and 12 mg of Al per gram of chondrite, the initial heat productions would be 2.6×10^{-8} and 2.5×10^{-7} W/kg, respectively, a tenfold difference. By the time the slower decay of ^{60}Fe allows it to dominate (~5 million years), heat production from both isotopes is inconsequential, $\sim 10^{-9}$ W/kg.
11. R. Greenberg and C. R. Chapman, *Icarus* **55**, 455 (1983).
12. J. Wisdom, *Nature* **315**, 731 (1985).
13. M. J. Gaffey and T. B. McCord, *Space Sci. Rev.* **21**, 555 (1978).
14. J. Gradie and E. Tedesco, *Nature* **216**, 1405 (1982).
15. J. F. Bell, D. R. Davis, W. K. Hartmann, M. J. Gaffey, in *Asteroids II*, R. P. Binzel, T. Gehrels, M. S. Matthews, Eds. (Univ. of Arizona Press, Tucson, 1989), pp. 921–945.
16. T. D. Jones, L. A. Lebofsky, J. S. Lewis, M. S. Marley, *Icarus* **88**, 172 (1990).
17. C. P. Sonett, D. S. Colburn, K. Schwartz, K. Keil, *Astrophys. Space Sci.* **7**, 446 (1970).
18. F. Herbert and C. P. Sonett, *Icarus* **40**, 484 (1979).
19. F. Herbert, *ibid.* **78**, 402 (1989).
20. F. A. Podosek *et al.*, *Geochim. Cosmochim. Acta* **55**, 1083 (1991).
21. G. J. MacPherson, A. M. Davis, E. K. Zinner, *Meteoritics* **27**, 253 (1992).
22. G. W. Wetherill, *Annu. Rev. Astron. Astrophys.* **18**, 77 (1980).
23. The surface density is given by $\sigma = M_c/4\pi a\,\Delta a$. For constant σ, $n = 3/2$; for $\sigma \sim a^{-1}$ (*28*), $n = 5/2$; and for $\sigma \sim a^{-3/2}$ (*35*), $n = 3$. The Titius-Bode geometrical progression of semimajor axes implies $\Delta a \sim a$, which also gives $n = 5/2$.
24. R. Greenberg, J. F. Wacker, W. K. Hartmann, C. R. Chapman, *Icarus* **35**, 1 (1978).
25. G. W. Wetherill and G. R. Stewart, *ibid.* **77**, 330 (1989).
26. P. Goldreich and W. R. Ward, *Astrophys. J.* **183**, 1051 (1973).
27. D. J. Stevenson, A. W. Harris, J. I. Lunine, in *Satellites*, J. Burns and M. S. Matthews, Eds. (Univ. of Arizona Press, Tucson, 1986), pp. 39–88.
28. G. W. Wetherill and C. R. Chapman, in *Meteorites and the Early Solar System*, J. F. Kerridge and M. S. Matthews, Eds. (Univ. of Arizona Press, Tucson, 1988), pp. 35–67.
29. S. J. Weidenschilling, *ibid.*, pp. 348–371.
30. J. A. Wood and G. E. Morfill, *ibid.*, pp. 329–347.
31. L. A. Lebofsky, M. A. Feierberg, A. T. Tokunaga, H. P. Larson, J. R. Johnson, *Icarus* **48**, 453 (1981).
32. T. E. Bunch and S. Chang, *Geochim. Cosmochim. Acta* **44**, 1543 (1980).
33. R. G. Prinn and B. Fegley, Jr., *Annu. Rev. Earth Planet. Sci.* **15**, 171 (1987).
34. J. Schubart and D. L. Matson, in (*1*), pp. 84–97.
35. S. J. Weidenschilling, *Astrophys. Space Sci.* **51**, 153 (1977).

3 September 1992; accepted 1 December 1992

Isotope Effect and Superconductivity in Metal-Doped C_{60}

Chia-Chun Chen and Charles M. Lieber*

The mechanism of superconductivity in alkali metal–doped fullerenes remains a fascinating and controversial issue. One powerful probe of this mechanism involves the determination of the shift in transition temperature (δT_c) upon isotopic substitution. A series of isotopically substituted Rb_3C_{60} superconductors, where C_{60} corresponds to $^{13}C_{60}$, $(^{13}C_{60})_{0.5}(^{12}C_{60})_{0.5}$, or $(^{13}C_{0.55}{}^{12}C_{0.45})_{60}$, was investigated. The δT_c determined for $Rb_3{}^{13}C_{60}$, 0.7 ± 0.1 K, provides an unambiguous value for the isotope shift in fully substituted fullerene superconductors. The δT_c determined for $Rb_3(^{13}C_{0.55}{}^{12}C_{0.45})_{60}$, 0.5 K, is also consistent with simple mass scaling of the $Rb_3{}^{13}C_{60}$ result. However, an intermolecular effect not accounted for in existing theories is demonstrated by the unexpectedly large δT_c, 0.9 K, that was observed for the $Rb_3(^{13}C_{60})_{0.5}(^{12}C_{60})_{0.5}$ materials. These results are used to critically assess proposed mechanisms of fullerene superconductivity.

Metal-doped fullerenes represent a fascinating class of superconductors that can exhibit transition temperatures (T_c) in excess of 30 K (*1–5*). The existence of superconductivity at such surprisingly high temperatures has led to considerable speculation about the mechanism of superconductivity and about the possibility of achieving higher temperature transitions. Theoretical models put forth to explain the formation of Cooper pairs and superconductivity in the fullerenes range from conventional electron-phonon models (*6–9*) to purely electronic mechanisms (*10, 11*). An important assumption in both of these models is that superconducting pair formation is dominated by the properties of single clusters and that the bulk T_c can be obtained from a conventional mean-field average of the single cluster properties. Because the coherence length of the superconducting pairs is so short (≈25 Å) in the fullerene superconductors and because it is uncertain whether intercluster terms can indeed be ignored, it remains essential to probe the contributions of both the single cluster and the intercluster contributions to superconductivity.

Department of Chemistry and Division of Applied Sciences, Harvard University, Cambridge, MA 02138.

*To whom correspondence should be addressed.

We address here the open question of the mechanism of superconductivity in the fullerenes through systematic investigations of a series of ^{13}C-substituted Rb_3C_{60} superconductors for which the isotopic substitution within the solid is precisely controlled. The classic phonon-mediated pairing model of Bardeen, Cooper, and Schrieffer (BCS) (*12*) predicts that $T_c \propto M^{-\alpha}$, where M is the ionic mass and α is the isotope shift exponent. For simple metals, α equals 0.5. Electron-electron interactions in real materials may reduce the value of α below 0.5 (*13, 14*). Measurements of the isotope shift in Rb_3C_{60} have been made on materials containing poorly controlled isotopic distributions and $^{12}C_{60}$ impurity (*15–17*). Ramirez and co-workers (*15*) found that $\alpha \approx 0.37$ in samples containing, on average, 75% ^{13}C, whereas two other groups (*16, 17*) reported that α was >1 in samples containing smaller percentages of ^{13}C. In all of these studies the value of α was determined by extrapolating to 100% $^{13}C_{60}$ with little regard for the detailed composition of the starting material. The conflicting values for these extrapolated isotope shifts have made conclusions about the absolute magnitude of α and the mechanism of superconductivity unclear. To determine unambiguously the magnitude of α for Rb_3C_{60} and to elucidate the essential role of intercluster versus intramolecular in-

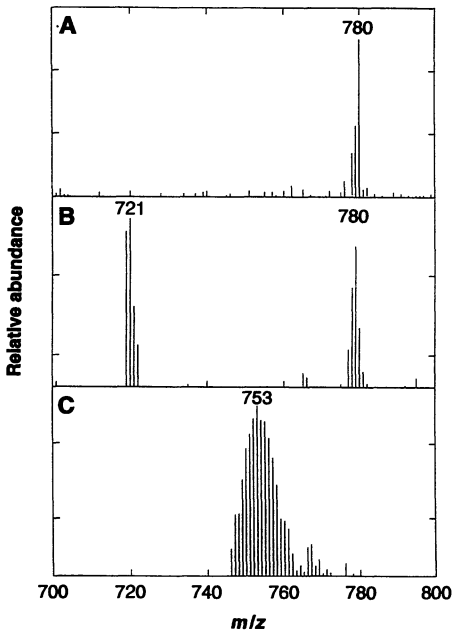

Fig. 1. Fast atom bombardment (FAB) mass spectra of purified samples of (**A**) $^{13}C_{60}$, (**B**) a 50:50 mixture of $^{13}C_{60}$ and $^{12}C_{60}$, and (**C**) $(^{13}C_{0.55}{}^{12}C_{0.45})_{60}$. The matrix used for the FAB experiments was 3-nitrobenzyl alcohol.

teractions in the fullerenes, we have characterized T_c in a series of Rb_3C_{60} superconductors for which C_{60} corresponds to $^{13}C_{60}$, $(^{13}C_{60})_{0.5}(^{12}C_{60})_{0.5}$, or $(^{13}C_{0.55}{}^{12}C_{0.45})_{60}$. We found that the shifts in T_c measured for $Rb_3{}^{13}C_{60}$ and $Rb_3(^{13}C_{0.55}{}^{12}C_{0.45})_{60}$, 0.7 K and 0.5 K, respectively, are consistent with both conventional phonon-mediated pairing and a recently proposed electronic mechanism (*10*, *18*). However, an unexpectedly large shift in T_c, 0.9 K, has been determined from investigations of the $Rb_3(^{13}C_{60})_{0.5}$-$(^{12}C_{60})_{0.5}$ materials. These latter results have not yet been accounted for by either electron-phonon or electronic mechanisms of superconductivity in the fullerenes.

We prepared the $^{13}C_{60}$ and $(^{13}C_{0.55}$-$^{12}C_{0.45})_{60}$ materials using an adaptation of our reported methodology (*19*). An essential feature of this procedure is that dense ^{13}C-substituted rods are obtained without the use of binders or preformed ^{12}C rods. In previous investigations, the use of binders and ^{12}C rods has led to uncontrolled isotope distributions. In our studies, either 99% ^{13}C powder or a mixture of ^{13}C and 99% ^{12}C powder was ground extensively, placed in a quartz tube between two tantalum electrodes, and then converted into dense carbon rods by resistive heating under pressure (*19*). We produced $^{13}C_n$ and $(^{13}C_{0.55}{}^{12}C_{0.45})_n$ fullerenes from the isotopically substituted carbon rods by laser ablation in an argon atmosphere at 1200°C (*20*). Approximately 5 mg of $^{13}C_{60}$ can be produced from 0.5 g of ^{13}C powder by these methods. We isolated the isotopically substituted C_{60} using well-established chromatographic procedures (*4*, *21*). Careful attention was paid to the purification of the C_{60} products because impurities (such as C_{70}) can depress T_c in the metal-doped superconductors. The purity of all of the isotopically substituted C_{60} products was verified by optical, mass, and nuclear magnetic resonance spectroscopies.

Figure 1 shows mass spectra of the purified, isotopically substituted C_{60} samples. The $^{13}C_{60}$ sample exhibits a M^+ signal at 780 atomic mass units (amu) characteristic of a fully substituted material (Fig. 1A). No peaks were observed above background in the regions 700 to 770 amu and 900 to 950 amu, and thus it is apparent that this material is not contaminated with either $^{12}C_{60}$ or $^{13}C_{70}$. The mixture of $^{13}C_{60}$ and $^{12}C_{60}$ shows peaks of approximately equal intensity at 720 and 780 amu (Fig. 1B). The $^{13}C_{60}/^{12}C_{60}$ mixture was prepared by combining toluene solutions of purified $^{13}C_{60}$ and $^{12}C_{60}$ of similar concentration and then evaporating the resulting solution; this procedure yielded a solid containing $^{13}C_{60}$ and $^{12}C_{60}$ randomly mixed on the molecular scale. The C_{60} product formed from a roughly 50:50 mixture of ^{13}C and ^{12}C exhibits a mass distribution with a peak at 753 amu corresponding to $(^{13}C_{0.55}$-$^{12}C_{0.45})_{60}$ (Fig. 1C). The full width at half maximum for this distribution is 8.9 amu. In contrast to previous studies (*15–17*), pure $^{12}C_{60}$ is not present in our intramolecular substituted materials.

We also characterized the infrared (IR) active modes in this series of isotopically C_{60} materials; the low-frequency modes for the three isotopically substituted samples are shown in Fig. 2. The IR spectrum of $^{13}C_{60}$ (Fig. 2A) exhibits the four IR-active modes of the C_{60} icosahedron shifted by the expected $(12/13)^{1/2}$ mass ratio. The spectrum of the $(^{13}C_{60})_{0.5}(^{12}C_{60})_{.05}$ mixture (Fig. 2B) exhibits eight peaks that can be assigned to a simple superposition of pure $^{12}C_{60}$ and pure $^{13}C_{60}$ spectra. The linewidths for the IR modes in this isotopic solid solution are the same as those in the pure $^{12}C_{60}$ and $^{13}C_{60}$ samples. The similarity of these linewidths indicates that intercluster vibrational coupling is not unusual in the $(^{13}C_{60})_{0.5}$-$(^{12}C_{60})_{0.5}$ materials. In addition, spectra recorded on the $(^{13}C_{0.55}{}^{12}C_{0.45})_{60}$ samples (Fig. 2C) exhibit four modes shifted by the average mass factor $0.6(12/13)^{1/2}$; this shift reflects the partial substitution of ^{13}C on each cluster. The broadening of the IR lines for this sample (versus $^{12}C_{60}$ or $^{13}C_{60}$) is consistent with the width of the sample mass distribution (Fig. 1C). These IR data are thus consistent with the mass spectral data; moreover, these results show that ^{13}C substitution results in conventional isotope shifts for the cluster vibrations.

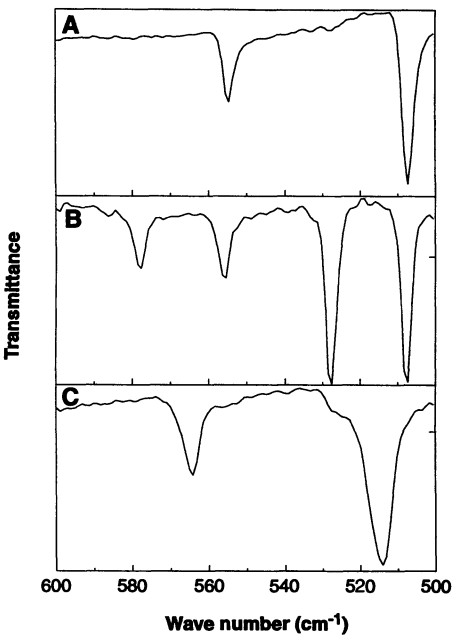

Fig. 2. The IR spectra of purified samples of (**A**) $^{13}C_{60}$, (**B**) a 50:50 mixture of $^{13}C_{60}$ and $^{12}C_{60}$, and (**C**) $(^{13}C_{0.55}{}^{12}C_{0.45})_{60}$. The spectra were recorded on C_{60} thin films, which we prepared by sublimation onto KBr pellets, using a Fourier transform IR spectrometer.

This series of well-characterized ^{13}C-substituted materials has been used to determine the isotope effect on superconductivity in the fullerenes. We prepared Rb_3C_{60} [$C_{60} = {}^{13}C_{60}$, $(^{13}C_{60})_{0.5}(^{12}C_{60})_{0.5}$, or $(^{13}C_{0.55}{}^{12}C_{0.45})_{60}$] materials by heating stoichiometric amounts of purified, solvent-free C_{60} with Rb metal (3:1, Rb:C_{60}) in sealed quartz tubes (*3*). Samples were reacted over a 3-day period while the temperature was increased from 300° to 350°C. Approximately 5 mg of C_{60} was used for each sample. The superconducting properties of these materials were assessed by dc-magnetization measurements (MPMS2, Quantum Design, San Diego, California). Typically, the diamagnetic shielding exhibited by the samples was in excess of 15% of the value predicted for complete shielding. Incomplete flux exclusion is expected for these polycrystalline samples because the grain size is similar to the penetration depth. Because the transition shape is also affected by the particle size of the samples, we have been careful to analyze magnetization data from samples with similar grain sizes (*22*).

The key magnetization data from this study are shown in Fig. 3. These results are representative of measurements made on more than 15 independent isotopically substituted Rb_3C_{60} samples. Comparison of the magnetization data for the ^{13}C-substituted materials versus $Rb_3{}^{12}C_{60}$ shows that there is a reproducible depression of T_c with

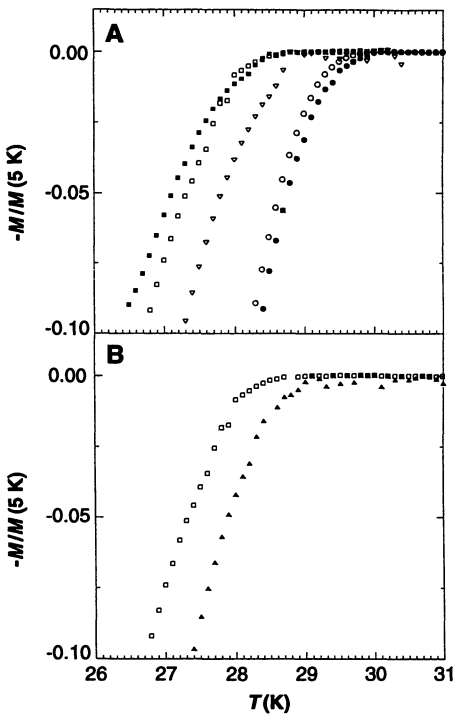

Fig. 3. (**A**) Comparison of the diamagnetic shielding versus temperature data recorded on $Rb_3{}^{12}C_{60}$ (○ and ●), $Rb_3{}^{13}C_{60}$ (▽), and $Rb_3(^{13}C_{60})_{0.5}(^{12}C_{60})_{0.5}$ (□ and ■) samples in a field of 10 Oe. (**B**) Comparison of the magnetization versus temperature data for $Rb_3(^{13}C_{0.55}{}^{12}C_{0.45})_{60}$ (▲) and $Rb_3(^{13}C_{60})_{0.5}(^{12}C_{60})_{0.5}$ (□) recorded in a field of 10 Oe. The data in (A) and (B) have been normalized to the magnetization at 5 K to accurately compare the different transition temperatures of the four compounds. We made the measurements by initially cooling the samples in zero field to 5 K; the data were then recorded on warming in a field of 10 Oe.

isotopic substitution. We have assigned the T_c of these materials to the temperature at which the magnetization deviates from the background susceptibility. Comparison of normalized curves with similar transition shapes provides a consistent and reproducible measure of T_c in these materials (*23*). The T_c (±1 SD) determined for the fully ^{13}C-substituted materials, $Rb_3{}^{13}C_{60}$, is 28.9 ± 0.1 K (Fig. 1A). The value of α for the completely substituted materials is thus 0.30 ± 0.05. This value of α is in good agreement with the value we reported recently (*19*) for 99% ^{13}C-substituted K_3C_{60}. Although it is possible that a slightly smaller isotope shift may be obtained in homogeneous single crystals (that is, the transition onset in a single crystal should not be rounded), we believe that this value of α represents a robust and unambiguous value for the isotope effect in the fully ^{13}C-substituted fullerene superconductors.

Important insight into the nature of superconductivity in the fullerenes is provided by our measurements on partially substituted materials. Specifically, the isotope shift for $Rb_3(^{13}C_{60})_{0.5}(^{12}C_{60})_{0.5}$ is larger than the shift observed for $Rb_3{}^{13}C_{60}$ (Fig. 3A). Measurements made on five independent samples yielded a shift in T_c (δT_c) of 0.9 ± 0.1 K. The reproducibility of these measurements strongly indicates that this δT_c is intrinsic to the $Rb_3(^{13}C_{60})_{0.5}(^{12}C_{60})_{0.5}$ materials. Furthermore, a 0.5 K isotope shift for $Rb_3(^{13}C_{0.55}{}^{12}C_{0.45})_{60}$, which contains an average mass substitution similar to that of $Rb_3(^{13}C_{60})_{0.5}(^{13}C_{60})_{0.5}$, is smaller than the shifts observed for either $Rb_3(^{13}C_{60})_{0.5}(^{12}C_{60})_{0.5}$ or $Rb_3{}^{13}C_{60}$ (Fig. 3B). These data demonstrate that complete isotopic substitution of a fraction of the clusters (that is, intermolecular substitution) is distinct from partial isotopic substitution of all of the clusters (that is, intramolecular substitution). The implications of these results are discussed below.

These data provide a clear value for the isotope effect in fully ^{13}C-substituted Rb_3C_{60}: δT_c = 0.7 ± 0.1 K and α = 0.30 ± 0.05. Furthermore, this result and our measurements of selectively substituted materials suggest a resolution of the conflicting values reported for the Rb_3C_{60} isotope shift. In previous investigations of Rb_3C_{60} samples containing partially substituted clusters and $^{12}C_{60}$, values of α (extrapolated to 100% isotopic substitution) ranging from 0.2 to >1 were reported (*15–17*). Our studies demonstrate that homogeneous samples consisting of partially substituted or completely substituted clusters do not exhibit an unusually large δT_c, although an intermolecular mix of $^{13}C_{60}$ and $^{12}C_{60}$ does lead to an anomalously large isotope effect in the fullerene superconductors. We thus believe that large isotope shifts can be attributed in general to samples containing a mixture of clusters with significant isotopic mass differences.

Our results can be used to evaluate critically existing models of fullerene superconductivity. Phonon-mediated pairing mechanisms have been reported by several groups (6–9). These models predict a conventional isotope effect ($T_c \propto M^{-\alpha}$) with $\alpha \leq 0.5$ or $\delta T_c \leq 1.2$ K for $Rb_3{}^{13}C_{60}$. At the other extreme, Chakravarty and co-workers have proposed an electronic model for pairing (*10, 18*). Interestingly, sizable isotope shifts, δT_c = 0.2 to 0.6 K for Rb_3C_{60}, have been predicted by this model as well (*18*). The isotope shift in this electronic mechanism arises from an increase in the intramolecular hopping matrix element due to decreases in the mean intramolecular C–C separation with increasing mass. It is apparent from a comparison of these theoretical predictions with our experimental data (Fig. 4) that the experimental δT_c obtained for the completely substituted material,

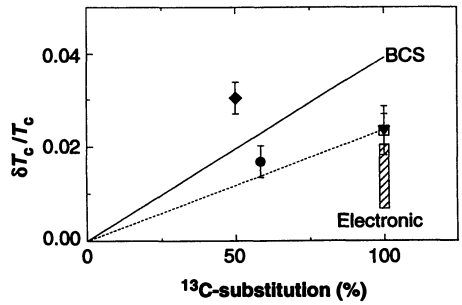

Fig. 4. Plot of the normalized isotope shift ($\delta T_c/T_c$) versus the percentage ^{13}C enrichment. The solid and dashed lines correspond to the behavior predicted for conventional (BCS) phonon-mediated pairing ($T_c \propto M^{-\alpha}$) with α = 0.5 and 0.3, respectively. The shaded bar corresponds to the range of isotope shift values predicted by the electronic pairing model of Chakravarty *et al.* (*18*) for 100% isotopic substitution. The experimental points are $Rb_3{}^{13}C_{60}$ (▼), $K_3{}^{13}C_{60}$ (□), $Rb_3(^{13}C_{0.55}{}^{12}C_{0.45})_{60}$ (●), and $Rb_3(^{13}C_{60})_{0.5}(^{12}C_{60})_{0.5}$ (◆). The bars on the experimental points correspond to the uncertainty (±1 SD) in the determination of δT_c.

$Rb_3{}^{13}C_{60}$, is consistent with the predictions of both the electron-phonon and the electronic models. The isotope shift for $Rb_3(^{13}C_{0.55}{}^{12}C_{0.45})_{60}$ is also consistent with phonon-mediated pairing; that is, the fractional shift in the average phonon frequency due to partial substitution simply reduces δT_c compared to the fully substituted materials. The δT_c for $Rb_3(^{13}C_{0.55}{}^{12}C_{0.45})_{60}$ may be consistent with the electronic mechanism because the average change in the intramolecular hopping matrix element per cluster, which determines δT_c, will be related to the fractional substitution of the clusters. Explicit calculations should be carried out, however, to verify that the electronic mechanism is consistent with our intramolecular ^{13}C-substitution data.

Importantly, the isotope shift results obtained from the $Rb_3(^{13}C_{60})_{0.5}(^{12}C_{60})_{0.5}$ samples are inconsistent with the predictions of both the electron-phonon and electronic pairing models. Intramolecular phonon-mediated pairing models (*6, 7*) predict that intermolecular $[(^{13}C_{60})/(^{12}C_{60})]$ and intramolecular $[(^{13}C_{0.55}{}^{12}C_{0.45})_{60}]$ isotopic substitution should yield similar results because the phonons responsible for pairing are averaged over the length scale of the pairs, 25 Å. This prediction clearly contrasts with our observed results. It may be possible, however, to modify the electron-phonon model to account for our data. For example, it is not clear that a mean-field average is appropriate in these short-coherence length materials. In addition, we believe that it would be interesting to explore the role of pair-breaking scattering in $Rb_3(^{13}C_{60})_{0.5}(^{12}C_{60})_{0.5}$ versus $Rb_3(^{13}C_{0.5}{}^{12}C_{0.5})_{60}$ solids. In the case of the electron-

ic mechanism it is not known whether the differences in the matrix elements corresponding to hopping on $(^{13}C_{0.5}{}^{12}C_{0.5})_{60}$ versus $^{13}C_{60}$ and $^{12}C_{60}$ clusters will give rise to significant variations in T_c, or whether these differences are averaged in the mean-field model used to estimate T_c. Calculations for the electronic model are needed to address this essential issue.

Our experimental isotope effect data obtained on a series of specifically substituted Rb_3C_{60} superconductors provide an unambiguous value for the isotope shift in completely substituted fullerene superconductors and elucidate a unique difference between intermolecular and intramolecular isotopic substitution. A theoretical understanding of these experimental results may lead to a single viable mechanism for superconductivity in the fullerenes.

REFERENCES AND NOTES

1. A. F. Hebard *et al.*, *Nature* **350**, 660 (1991).
2. M. J. Rosseinsky *et al.*, *Phys. Rev. Lett.* **66**, 2830 (1991).
3. K. Holczer *et al.*, *Science* **252**, 1154 (1991).
4. C.-C. Chen, S. P. Kelty, C. M. Lieber, *ibid.* **253**, 886 (1991).
5. K. Tanigaki *et al.*, *Nature* **352**, 222 (1991).
6. C. M. Varma, J. Zaanen, K. Raghavachari, *Science* **254**, 989 (1991).
7. M. Schluter, M. Lannoo, M. Needels, G. A. Baraff, D. Tomanek, *Phys. Rev. Lett.* **68**, 526 (1992).
8. I. I. Mazin *et al.*, *Phys. Rev. B* **45**, 5114 (1992).
9. D. L. Novikov, V. A. Gubanov, A. J. Freeman, *Physica C* **191**, 399 (1992).
10. S. Chakravarty, M. P. Gelfand, S. Kivelson, *Science* **254**, 970 (1991).
11. G. Baskaran and E. Tossatti, *Curr. Sci.* **61**, 33 (1991).
12. J. Bardeen, L. N. Cooper, J. R. Schrieffer, *Phys. Rev.* **108**, 1175 (1957).
13. P. Morel and P. W. Anderson, *ibid.* **125**, 1263 (1962).
14. W. L. McMillan, *ibid.* **167**, 331 (1968).
15. A. P. Ramirez *et al.*, *Phys. Rev. Lett.* **68**, 1058 (1992).
16. T. W. Ebbesen *et al.*, *Nature* **355**, 620 (1992).
17. A. A. Zakhidov *et al.*, *Phys. Lett. A* **164**, 355 (1992).
18. S. Chakravarty, S. A. Kivelson, M. I. Salkola, S. Tewari, *Science* **256**, 1306 (1992).
19. C.-C. Chen and C. M. Lieber, *J. Am. Chem. Soc.* **114**, 3141 (1992).
20. Y. Chai *et al.*, *J. Phys. Chem.* **95**, 7564 (1991).
21. F. Diederich *et al.*, *Science* **252**, 548 (1991).
22. We prepared materials with similar grain sizes by using identical procedures to isolate the isotopically substituted C_{60} solids from solution and to dope these solids with Rb.
23. It is also possible to define T_c as the point of maximum curvature in the magnetization data (*15*). Analysis of our data using this definition yields isotope shifts that are similar to the values reported in the text.

24. We acknowledge helpful discussions with P. Allen, M. Tinkham, and E. Kaxiras. We thank E. Mazur and J.-K. Wang for helpful advice during the initial stages of the laser ablation experiments, and A. N. Tyler for the mass spectroscopy measurements. C.M.L. acknowledges partial support of this work by the David and Lucile Packard Foundation. The mass and nuclear magnetic resonance spectroscopy facilities are supported by grants from NIH and NSF.

11 September 1992; accepted 25 November 1992

Element-Specific Magnetic Microscopy with Circularly Polarized X-rays

J. Stöhr, Y. Wu, B. D. Hermsmeier, M. G. Samant, G. R. Harp, S. Koranda, D. Dunham, B. P. Tonner

Circularly polarized soft x-rays have been used with an imaging photoelectron microscope to record images of magnetic domains at a spatial resolution of 1 micrometer. The magnetic contrast, which can be remarkably large, arises from the fact that the x-ray absorption cross section at inner-shell absorption edges of aligned magnetic atoms depends on the relative orientation of the photon spin and the local magnetization direction. The technique is element-specific, and, because of the long mean free paths of the x-rays and secondary electrons, it can record images of buried magnetic layers.

Polarized light has long been used to probe the magnetic properties of matter in the visible spectral range. Two prominent methods for examining the magnetic properties of solids are based on observing changes in light polarization upon reflection, the magneto-optical Kerr effect, or upon transmission, the Faraday effect (*1*). Because the energy of visible light is a few electron volts, the Kerr and Faraday effects involve electronic transitions from the valence to the conduction band. In the late 1980s, Schütz and co-workers demonstrated (*2*) that circularly polarized x-rays may also be used as a probe of magnetism. In the so-called magnetic circular x-ray dichroism (MCXD) technique, the difference in absorption between right and left circularly polarized x-rays is measured at an inner-shell absorption edge in magnetic materials. The uniqueness of the technique lies in the elemental specificity afforded by tuning to the characteristic atomic absorption edges. For transition metals, MCXD measurements typically involve p to d core-to-valence excitations near L_3 or L_2 edges (*2–4*).

We describe here the use of the MCXD technique for magnetic imaging. We have recorded pictures of magnetic bits on a CoPtCr magnetic recording disk with a lateral resolution of 1 μm obtained by use of circularly polarized soft x-rays with energies near the Co L_3 (778 eV) and L_2 (793 eV) edges and by detection and imaging of the secondary electrons from the sample with a photoemission microscope (*5*). Our results show that the contrast is remarkably large, such that images can be recorded without background subtraction. Our results were obtained on disks with protective overcoats of 130 Å of carbon and about 40 Å of an organic fluorocarbon lubricant, which emphasizes the power of the technique for technological applications. Besides being element-specific, MCXD microscopy has the advantage over conventional Kerr microscopy (*1*) that its diffraction-limited lateral resolution is tens rather than thousands of angstroms (*6*). We anticipate by straightforward extrapolation that it will be possible to achieve a lateral resolution of around 100 Å by 100 Å with state-of-the-art electron imaging systems (*7*) and enhanced x-ray intensities from insertion devices on electron storage rings (*8*).

The experiments were performed at the Stanford Synchrotron Radiation Laboratory (SSRL). X-ray absorption spectra with linearly polarized x-rays were recorded on the wiggler beamline 10-1, and the MCXD measurements were carried out on the bending magnet beamline 8-2, both of which are equipped with spherical grating monochromators. We obtained circularly polarized x-rays by moving an aperture and the prefocusing mirror below the plane of the electron orbit, yielding a degree of circular polarization of $(I^R - I^L)/(I^R + I^L) = 90 \pm 5\%$, where I^R and I^L are the x-ray intensities with right and left circular polarization, respectively. For the MCXD spectra two pieces cut from the same sample were remanently magnetized parallel to the surface but in opposite directions. Spectra were recorded at a grazing x-ray incidence angle of 20° with the photon spin of the right circularly polarized x-rays aligned either parallel or antiparallel to the magnetization direction of the two samples, respectively.

In the MCXD microscopy experiments we used an ultrahigh-vacuum–compatible photoelectron microscope based on secondary electron yield detection (width of kinetic energy distribution about 6 eV) (*5*). The device has a two-stage electrostatic lens system with a contrast aperture in the back-focal plane of the objective lens. The magnified image of the sample (adjustable field

J. Stöhr, Y. Wu, M. G. Samant, G. R. Harp, Almaden Research Center, IBM Research Division, 650 Harry Road, San Jose, CA 95120.
B. D. Hermsmeier, IBM San Jose, 5600 Cottle Road, San Jose, CA 95153.
S. Koranda, D. Dunham, B. P. Tonner, Synchrotron Radiation Center, University of Wisconsin–Madison, Stoughton, WI 53589.